Sound Generation by Ducted Flames

U.G. Hegde,* D. Reuter,† and B. T. Zinn‡
Georgia Institute of Technology, Atlanta, Georgia

The sound field established by a v-shaped flame confined in a rectangular duct is investigated both theoretically and experimentally. A theoretical model is developed to predict pressure spectra caused by the unsteady heat release from the flame. Comparisons between the theoretical and experimentally measured spectra confirm the validity of the model and are also reported. It is also found that changes in the flowfield in the flame zone can significantly modify combustion rates. These modifications, in turn, affect the generated sound field and are important in determining the pressure levels in the duct. The results of this investigation are applicable to combustion noise and instability studies in a variety of burner and propulsion system configurations.

Nomenclature

a = duct width
b = duct height
B = constant defined by Eq. (17)
B_1 = constant defined by Eq. (18)
c = speed of sound
C_p = specific heat at constant pressure
G = Green's function
k_{oo} = modified wave number
L = length of duct
L_1 = length of duct from entrance to flame zone
$\bar{M}_o$ = steady-state Mach number at duct inlet
$\bar{M}_L$ = steady-state Mach number at duct exit
q = heat release rate per unit volume
R = gas constant
S_{pp} = pressure autospectrum
S_{qq} = unsteady heat release rate autospectrum
S_{rr} = CH radiation autospectrum
t = time
T = temperature
$\bar{T}_o$ = steady-state cold gas temperature
$\bar{T}_f$ = steady-state flame temperature
u = velocity
x, x_o = axial coordinate
X = axial separation of flame holders
y = vertical coordinate direction
Y = vertical separation of flame holders
z = transverse coordinate
$Z_o, \hat{Z}_o$ = unmodified and modified specific acoustic impedances at entrance to duct
$Z_L, \hat{Z}_L$ = unmodified and modified specific acoustic impedances at exit of duct
α = defined by Eq. (14)
β = defined by Eq. (14)
ψ = specific acoustic admittance of duct side walls
δ = Dirac delta function
γ = ratio of specific heats
ω = angular frequency
χ = wall loss factor (per unit length)
λ = acoustic wavelength

Subscripts

ω = Fourier component
1 = relating to the region upstream of the combustion zone
2 = relating to the region downstream of the combustion zone

Superscripts

$-$ = time or ensemble average
$'$ = time dependent part (fluctuation)
$*$ = complex conjugate

Other

$< >$ = cross section average

Received April 20, 1987; revision received July 24, 1987.

*Research Engineer, School of Aerospace Engineering. Member AIAA.
†Graduate Research Assistant, School of Aerospace Engineering. Member AIAA.
‡Regents' Professor, School of Aerospace Engineering. Fellow AIAA.

I. Introduction

SOUND generated by unsteady combustion processes is of interest in several applications including propulsion devices, industrial furnaces, burners, and heaters. In the majority of cases, the generated sound is undesirable; for example, in ramjet engines, the problem may become so severe that unstable operation of the engine may occur.[1] In some cases, however, as in pulse combustors, sound pressure variations are essential to maintain operation.[2]

Unsteady combustion processes generate sound as a result of unsteady expansion of the fluid undergoing reaction. Depending upon the nature of the flowfield and the combustion process, unsteady combustion may arise in different ways. For example, the injection of fuel or combustible mixture may be unsteady, the flowfield may be turbulent, or there may be feedback of the acoustic motions on the flame.

For the purposes of this paper, confined flames are categorized as those burning in an enclosure and unconfined flames are those burning in a free space. In addition, a flame may be termed acoustically compact at a particular frequency if the corresponding acoustic wavelength is much larger than the extent of the combustion region. These distinctions are important in characterizing the generated sound field. Thus, for unconfined flames, the radiated sound field is (at least in the compact limit)[3] nondirectional and monopole in character.[4] For confined flames, on the other hand, reflections from the boundaries and wave guide effects can cause preferred directionality of the acoustic motions as well as sustain discrete frequency or narrow-band excitation around the natural frequencies of the enclosure.

There have been several recent investigations of combustion-generated sound. Strahle[5,6] has developed a general theory of combustion-generated noise for free flames in the low-frequency (acoustically compact) limit and shown that the radiated sound pressure is related to the time derivative of the heat release rate averaged over the combustion region. The generated sound in such cases is generally broadband with a frequency content related to the temporal variations in volume of the combustion region. Experimental verification of the theory has been obtained by Shivasankara et al.[7]

Sound generated by confined flames has been studied in relation to combusion instabilities in rocket motors and ramjets. A review is provided by Barrere and Williams.[8] A recent experimental investigation of noise sources in a ramjet-like combustor is presented by Ponsot et al.[9] The investigation presented here is also part of a larger research effort on combustion instabilities in dump-type ramjet combustors.[10]

In this paper, a theory for predicting the sound generated by flames enclosed in a duct is developed. Knowledge of the heat release rates from the flame is presumed and attention is focused on longitudinal wave motions. This is presented in Sec. II, "Theoretical Considerations." The theory is tested in an experimental setup in which a v-shaped flame is stabilized in a rectangular duct. Measurements are made of the unsteady heat release from the flame, in terms of emitted radiation, for input into the model. The calculated pressure spectra in the duct are then compared with experimentally measured spectra to test the theory, and good agreement is obtained. These results are presented in the Sec. III, "Experimental Efforts." In addition, the relationship between the frequency content of the unsteady combustion and the generated sound is investigated. It is also shown that the combustion rates are sensitive to changes in the flowfield in the flame region and, in turn, affect the generated sound levels.

II. Theoretical Considerations

Consider a rectangular duct similar to the one in Fig. 1. The x-axis is parallel to the duct axis, and the cross-sectional dimensions are a and b. The length of the duct is L. A premixed flow of reactants is introduced at $x = 0$ and the combustion occurs in a region ΔL_1 around L_1. The Mach number of the flow is assumed to be small (i.e., $\bar{M}^2 \ll 1$). A typical axial temperature profile which might be present in the duct is also shown in Fig. 1. Because of heat conduction upstream of the combustion region, there is a gradual rise in temperature from the cold temperature $\bar{T}_o$ at $x = 0$. A sharp rise in temperature occurs in the combustion zone to the flame temperature $\bar{T}_f$. Downstream of the combustion region, the temperature may again drop due to heat loss to the duct walls.

The wave equation for the pressure fluctuations in the duct will be briefly formulated. The pressure fluctuations will be assumed to be small with respect to the mean (i.e., steady-state) pressure levels allowing the application of the linearized conservation equations to obtain the required solutions. In addition, the actual details of the mean velocity field in the duct will be ignored. There are two reasons why this is permissible. First, the Mach number is taken to be small, so that convective effects in the wave equation may be ignored. Second, although the flowfield is instrumental in determining the combustion rates, the actual details of this process are not considered herein, and the needed reaction rates will be assumed known. Thus, it is assumed that the effects of the flowfield on the generated sound will be obtained implicitly through the unsteady combustion process. Significant effects on the sound field, only by virtue of changes in the flowfield which do not affect the reaction rates, are not expected. This approach is justified by the fact that unsteady combustion is a monopole acoustic source and is a much more efficient sound source than pure flow noise sources which are either quadrupole or dipole in character.[11] In addition, experimental results obtained as part of this investigation, and discussed in the next section, are in agreement with the model predictions.

Neglecting viscous and heat conduction effects (although mean temperature and density gradients are allowed) and assuming a perfect gas behavior, the linearized conservation equations can be expressed in the following form:

Continuity:

$$\frac{\partial \rho'}{\partial t} + \bar{\rho}\ \nabla \cdot \boldsymbol{u}' + \boldsymbol{u}' \cdot \nabla \bar{\rho} = 0 \tag{1}$$

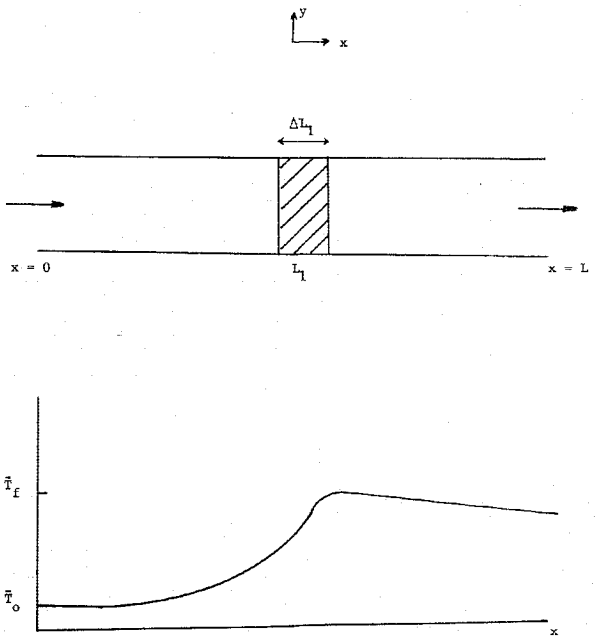

Fig. 1 Schematic of duct with a typical temperature distribution.

Momentum:

$$\bar{\rho}\frac{\partial \boldsymbol{u}'}{\partial t} = -\nabla p' \tag{2}$$

Energy:

$$\bar{\rho} C_p \left[\frac{\partial T'}{\partial t} + \boldsymbol{u}' \cdot \nabla \bar{T}\right] = \frac{\partial p'}{\partial t} + q' \tag{3}$$

State:

$$p' = R\bar{T}\rho' + R\bar{\rho}\ T' \tag{4}$$

Equation (1) may be rewritten in terms of p', u' and q' by substituting for T' and ρ' from Eqs. (3) and (4) and making use of the steady-state equation of state

$$\bar{p} = R\bar{\rho}\bar{T} \tag{5}$$

yielding

$$\frac{1}{c^2}\frac{\partial p'}{\partial t} + \bar{\rho}\nabla \cdot \boldsymbol{u}' = \frac{q'}{C_p \bar{T}} \tag{6}$$

where $c^2 = \gamma R\bar{T}$

Taking the divergence of Eq. (2) and subtracting the partial time derivative of Eq. (6) one obtains

$$\nabla \cdot (\bar{T}\ \nabla p') - \frac{\bar{T}}{c^2}\frac{\partial^2 p'}{\partial t^2} = \frac{-1}{C_p}\frac{\partial q'}{\partial t} \tag{7}$$

Equation (7) is the relevant wave equation for the pressure, taking into account the heat release from the combustion process and the spatial variations of the temperature. Harmonic motion is considered so that the fluctuations may be written in the form

$$p' = p_\omega\, e^{i\omega t} \text{ and } q' = q_\omega\, e^{i\omega t}$$

Substituting these solutions into Eq. (7) one obtains

$$\nabla \cdot (\bar{T}\nabla p_\omega) + \bar{T}\frac{\omega^2}{c^2} p_\omega = \frac{-i\omega}{C_p} q_\omega \tag{8}$$

Attention is now focused only on longitudinal wave motion. The axial wave equation may be obtained by integrating Eq. (8) over the duct cross section. Noting that $\bar{T}/c^2$ is independent of the location, it will be assumed that it may be replaced by $<\bar{T}>/<c^2>$. Also, for longitudinal wave motions, it is permissible to replace

$$\frac{\partial}{\partial x}\frac{1}{ab}\int\int \bar{T}\frac{\partial p_\omega}{\partial x}\,dy\,dz \quad \text{by} \quad \frac{d}{dx}<\bar{T}>\frac{d<p_\omega>}{dx}$$

as $p_\omega \equiv <p_\omega>$

Then, for longitudinal wave motion, Eq. (8) may be expressed as follows:

$$\frac{d}{dx}<\bar{T}>\frac{d}{dx}<p_\omega> + <\bar{T}><k_{oo}{}^2><p_\omega> = \frac{-i\omega}{C_p}<q_\omega> \tag{9}$$

where $<k_{oo}{}^2> = \left[\frac{\omega^2}{<c^2>} - i\frac{2\omega}{<c>}\frac{\psi(a+b)}{ab}\right]$

and ψ is the specific acoustic admittance of the side walls of the duct and is assumed to be independent of location along the duct. For rigid-walled ducts, this admittance is zero. For nearly rigid walls, as is considered here, the admittance remains small, and the modified wave number $<k_{oo}>$ may be approximated by[12]

$$<k_{oo} = \frac{\omega}{<c>} - i\chi$$

where χ is known as the wall loss factor.

Removing the now superfluous $<\ >$, Eq. (9) may be written as

$$\frac{d}{dx}\bar{T}\frac{dp_\omega}{dx} + \bar{T}k_{oo}{}^2 p_\omega = \frac{-i\omega}{C_p}q_\omega \tag{10}$$

where it is now understood that cross-sectional averages of quantities are under consideration.

The boundary conditions at $x = 0$ and $x = L$ may be written in terms of the specific acoustic impedances Z_o and Z_L at these two planes. It should be noted that, although convection effects may be negligible in determining the wave structure at low Mach numbers, convection losses at the end planes may be important in determining the amplitudes of the motions. This may be incorporated as shown in Ref. 13, and the relevant boundary conditions are

at $x = 0$:

$$\frac{dp_\omega}{dx} + \frac{i\,k_{oo}}{Z_o + M_o}p_\omega = 0$$

at $x = L$:

$$\frac{dp_\omega}{dx} + \frac{i\,k_{oo}}{Z_L + M_L}p_\omega = 0$$

The solution to Eq. (9) may be obtained in terms of the Green's function $G(x,x_o)$ satisfying

$$\frac{d}{dx}\bar{T}\frac{dG}{dx} + \bar{T}k_{oo}{}^2 G = -\delta(x - x_o) \tag{11}$$

along with the same boundary conditions as for p_ω. The solution for p_ω may then be written as

$$p_\omega(x) = \int_o^L \frac{i\omega q_\omega}{C_p}G(x,x_o)\,dx_o \tag{12}$$

An analytical solution will now be obtained for the important case when the length of the combustion zone, ΔL_1, is much smaller than the acoustic wavelength, λ. In such cases, the combustion zone may be treated as a discontinuity at $x = L_1$ as far as the acoustics are concerned. The unsteady heat release rate $q_\omega(x)$ may then be written as

$$q_\omega = q_\omega(x)\,\delta\,(x - L_1)$$

and the corresponding solution for p_ω becomes

$$p_\omega(x) = \frac{i\omega q_\omega(L_1)\,G(x,L_1)}{C_p} \tag{13}$$

The Green's function $G(x,L_1)$ may be obtained from Eq. (11) by setting $x_o = L_1$. The required jump conditions across the discontinuity at L_1 are i) G is continuous at L_1 and ii)

$$\bar{T}\frac{dG}{dx}\bigg|_{L_{1+}} + \bar{T}\frac{dG}{dx}\bigg|_{L_{1-}} = -1$$

The second condition is obtained by integrating Eq. (11) across L_1.

In general, most of the steady-state temperature change will occur in the combustion region as shown in Fig. 1. This change is accounted for in the matching conditions across the flame zone. The changes in the steady-state temperature away from the combustion zone will now be accommodated in an approximate fashion to simplify the computations. Upstream and downstream of the combustion zone, constant (although different) average temperatures will be prescribed. Thus, in the region $0<x<L_1$, the steady-state temperature is taken to be $\bar{T}_1$ (approximately equal to the cold gas temperature) and in the region $L_1<x<L$, the steady-state temperature is taken to be $\bar{T}_2$ (aaproximately equal to $\bar{T}_f$, the flame temperature, provided heat losses to the walls are not significant).

The comparison with the experimental pressure spectrum will be made at $x = 0$. The Green's function $G(0,L_1)$ may be obtained by standard methods[12] and it turns out to be

$$G(0,L_1) = \frac{-[\hat{Z}_o][\hat{Z}_L\cos\beta + i\sin\beta]}{[k_1\bar{T}_1[\hat{Z}_o\sin\alpha + i\cos\alpha][\hat{Z}_L\cos\beta + i\sin\beta]} \\ \overline{-k_2\bar{T}_2[-\hat{Z}_L\sin\beta + i\cos\beta][\hat{Z}_o\cos\alpha - i\sin\alpha]]} \tag{14}$$

where

$$\alpha = (k_{oo})_1\,L_1,\ \beta = (k_{oo})_2\,(L_2 - L_1),\ k_1 = (k_{oo})_1,\ k_2 = (k_{oo})_2$$

with (k_{oo}) and $(k_{oo})_2$ being the relevant wave numbers upstream and downstream of the flame region and the modified impedances $\hat{Z}_o$ and $\hat{Z}_L$ are given by

$$\hat{Z}_o = Z_o + \bar{M}_o \text{ and } \hat{Z}_L = Z_L + \bar{M}_L$$

The pressure spectrum S_{pp} is obtained by multiplying Eq. (13) by its complex conjugate and taking an ensemble average. The result is (for $x = 0$)

$$S_{pp}(x = 0) = \frac{\omega^2}{C_p{}^2}\left|G(0_1L_1)\right|^2 S_{qq}(x = L_1) \tag{15}$$

where S_{qq} is the spectrum of the unsteady heat release from the combustion region.

The natural frequencies of the duct may be obtained by minimizing the magnitude of the denominator of the Green's function. For example, consider the case of a rigid walled duct with no convection losses, which is acoustically rigid at $x = 0$ (i.e., $\hat{Z}_o = \infty$) and open at the end $x = L$ (i.e., $\hat{Z}_L = 0$). In this case, the natural frequencies are given by the relation

$$\cos(\alpha + \beta) + [\sqrt{\bar{T}_2/\bar{T}_1} - 1][\cos\alpha\cos\beta] = 0 \tag{16}$$

III. Experimental Efforts

The experimental setup used is shown in Fig. 2. It consists of a rectangular duct three meters long. It has a 7.5×5 cm^2 cross section and consists of an inlet, combustor, and exhaust section. The inlet contains an injector whose face is made of sintered stainless steel. A mixture of propane and air is introduced into the set up via the injector. A v-shaped flame is stabilized in the combustor section on a 0.8 mm diam nichrome wire. The wire is attached to the combustor windows at half combustor height, and it is heated electrically to improve its flame-holding characteristics. The windows are made of quartz and allow optical access to the flame zone.

The flow approaching the stabilizing wire is parallel and uniform, and a fine wire mesh grid located 8 cm upstream of the stabilizing wire acts as a flame arrestor in case of a flashback. The cold-flow Reynolds number is kept below 10,000 in the interest of maintaining a disturbance free flow. Typical cold-flow velocities considered are in the range of 1–2 m/s. The combustor walls are water cooled, enabling wall-mounted pressure transducers to be used to monitor the acoustic pressure field. In addition, temperature measurements are carried out by means of thermocouple junctions.

Capabilities for measuring spontaneous CH species radiation from the flame have also been developed. The concentrations of these species are a measure of the reaction rate,[4,14] and thus the heat release rate, and are useful in describing the unsteady combustion field. Consequently the autospectrum of the unsteady heat release rate is proportional to that of the radiation and the following relation is assumed to hold

$$S_{qq} = B\, S_{rr} \tag{17}$$

where B is a positive, real constant.

The radiation signal was measured from the entire flame to obtain the net unsteady heat release spectrum from the combustion zone. The autospectrum of a typical measurement is shown in Fig. 3. According to Eqs. (15) and (17) this spectrum may be regarded as the source for the corresponding pressure fluctuations. Note that the spectrum is dominated by low frequency components. Detailed investigations of the flame region are presented in Ref. 10 where it is shown that this pattern occurs because of the dominating influence of large scale structures in the flame region.

Measurements of the radiation signal from the flame were carried out under several different conditions. The fuel fraction was changed between approximately 2.1% to 2.4%. Measurements at higher fuel fractions could not be made due to the appearance of combustion instability in the system which resulted in flame flashback (see Ref. 10). Measured flame temperatures were in the 1250 to 1400°K range. Experiments were also run in a shortened version of the setup shown in Fig. 2 by removing the exhaust section. This had the effect of increasing the natural frequencies of the setup. In addition, some experiments were performed in the presence of an additional flame holder in the combustor section. This served to modify the flowfield in the flame region and addressed the question whether the flowfield influences the sound generation process in a direct fashion (i.e., is the sound field changed appreciably by the flowfield even without changes in the unsteady heat release rate?). This question will be discussed shortly.

To carry out the theoretical calculations of the pressure spectra, the values of $\hat{Z}_o$, $\hat{Z}_L$, the wall loss factor χ and the constant B [Eq. (17)] must be known. Impedance measurements in cold-flow (i.e., flow without combustion) tests using an impedance tube technique and an available computer program indicated that the setup behaved to a good approximation as an acoustically closed-open duct. Thus, $\hat{Z}_L$ and $1/\hat{Z}_o$ were both set to zero. The wall loss factor χ was modeled, following Pierce,[15] as

$$\chi = B_1\, \omega^{0.5} \tag{18}$$

where B_1 is a constant, independent of the frequency and depends only upon the characteristics of the duct walls.

To estimate B_1 and B, a trial-and-error technique was used. A sample pressure and corresponding radiation spectrum were chosen. Using Eqs. (15) and (17), theoretical pressure spectra corresponding to different values of B_1 and B were calculated. The values of B_1 and B yielding the best fit with the experimental pressure spectrum were determined. Once determined, B_1 and B are known for all the tests run on the experimental setup, since they depend only upon the duct and radiation data acquisition system characteristics (which remained the same in all the tests).

The comparison between the theoretical and experimental pressure spectra correspoinding to the radiation spectrum in Fig. 3 is shown in Fig. 4. Using the same values of B and B_1 (recall the wall loss factor is defined for unit length and remains the same), a comparison between the theoretical and experimental pressure spectra for the shortened-duct case is shown in Fig. 5. The unsteady radiation spectrum measured for this case is shown in Fig. 6. The agreement in both these cases and for all the other cases tried (but not shown here for brevity) is very good and serves to verify the theory. Note that the comparison is made only in the low-frequency range (up to approximately 250 Hz). In this frequency range, the flame zone length (of the order of 20 cm) is an order of magnitude smaller than the relevant acoustic wavelengths.

Some comments are in order regarding the connection between the frequency content of the source (the unsteady heat release rate) and the pressure fluctuations. The unsteady heat release is broadband in nature (see Figs. 3 and 6) with low-frequency components dominating (frequencies less than

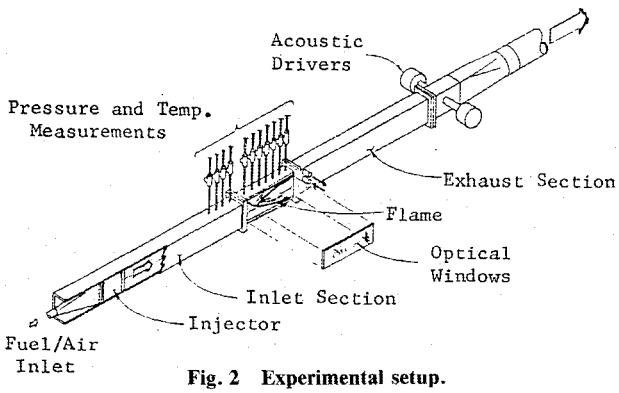

Fig. 2 Experimental setup.

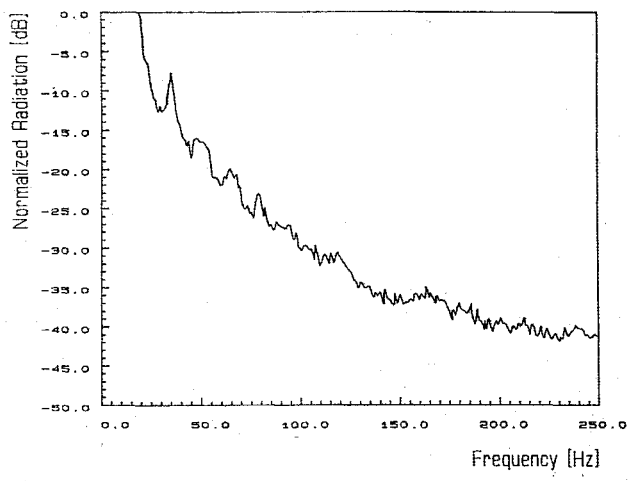

Fig. 3 Autospectrum of measured radiation (long duct).

approximately 100 Hz in the considered experiments). As shown in Ref. 10, this behavior is due to the presence of large-scale structures in the flame region. For an unenclosed flame, this frequency content is reflected in the resulting pressure fluctuations, which also are broadband in nature.[5] For enclosed flames, however, such as those considered here, the pressure spectrum is modified by the presence of the duct natural frequencies. Theoretically, this may be explained in terms of the Green's function G and the requirement that the frequency spectrum of the time rate of variation of the heat release rate [the source for the pressure fluctuations, see Eq. (7)] be bounded. The latter requirement implies that $\overline{(\partial q/\partial t)(\partial q/\partial t)^*}$ varies approximately as ω^{-n} where n is a positive number. This implies that $\omega^2 S_{qq}$ also varies as ω^{-n}. Thus, the frequency dependence of the pressure spectrum may be given by [see Eq. (15)]

$$S_{pp} \sim \omega^{-n} \left| G \right|^2$$

As noted earlier, Green's function G is maximized at the natural frequencies of the duct. However, the presence of ω^{-n} ensures that the pressure fluctuations also exhibit an upper cutoff, and only the first few natural frequencies will be significant in the sprectrum.

The theory constructed herein is valid for any flame shape in the combustion region, as long as this region is compact compared to the relevant acoustic wavelength. The flame shape is largely dependent upon the nature of the flowfield in the combustion region. In the theory, the flow effects are not included directly but are included implicitly in the unsteady heat release (which is controlled by the flow to a large extent) which is presumed known. Thus, it is assumed that the sound pressure fluctuations are mainly affected by changes in the unsteady heat release (which is controlled by the flow to a large extent) which is presumed known. Thus, it is assumed that the sound pressure fluctuations are mainly affected by changes in the unsteady heat release and are not directly modified by the flowfield (i.e., the effect of the flowfield is indirect via the unsteady heat release). To check this assumption, the flame shape was changed by introducing a second flame holder into the combustion region as shown in Fig. 7. This second flame holder was a cylindrical rod, 5 mm in diameter, and its introduction resulted in the formation of a double v-shaped flame. The position of this flame holder could be adjusted with respect to the original flame holder (i.e., the wire). Thus, several different combustion zones could be investigated.

As an example, consider a set of experiments in which the vertical displacement Y between the flame holders was held fixed while the axial displacement X was varied. It was found that, depending upon the distance, X, the pressure levels measured at $x = 0$ varied between 100 to 140 dB. However, in all cases, the changes in the pressure levels were linearly related to the changes in the radiation levels. This is shown in Fig. 8, which plots the obtained pressure levels as a function of the corresponding radiation levels at the first natural frequency. The predicted pressure spectra were also found to be in good agreement with the experimentally measured spectra in all cases. These experiments, therefore, verify the assumption inherent in the theoretical model, that changes in the flowfield affect the generated sound mainly by changing the associated combustion rates and not in a direct manner.

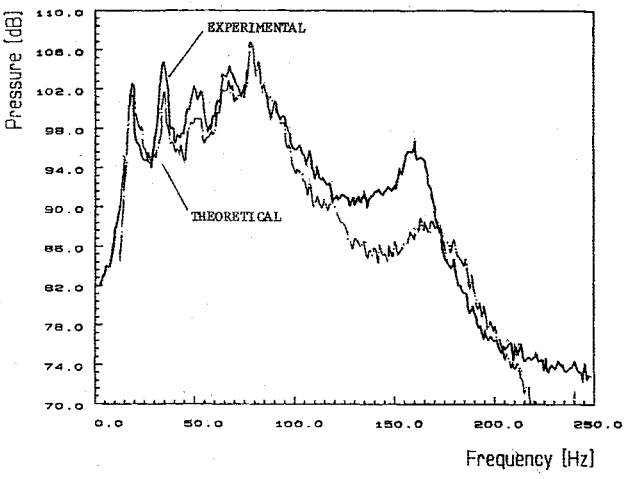

Fig. 4 Comparison of experimental and theoretical pressure spectra (long duct).

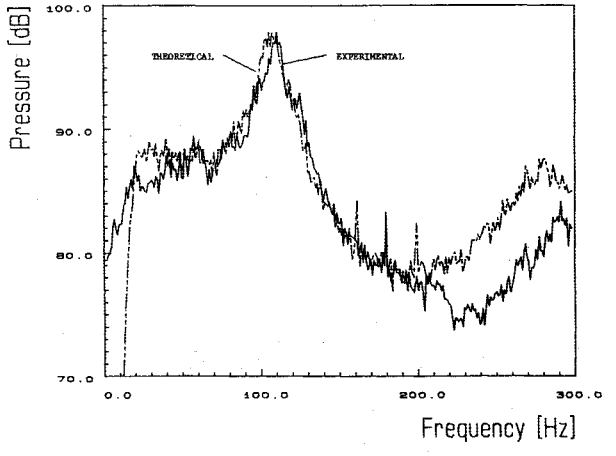

Fig. 5 Comparison of experimental and theoretical pressure spectra (short duct).

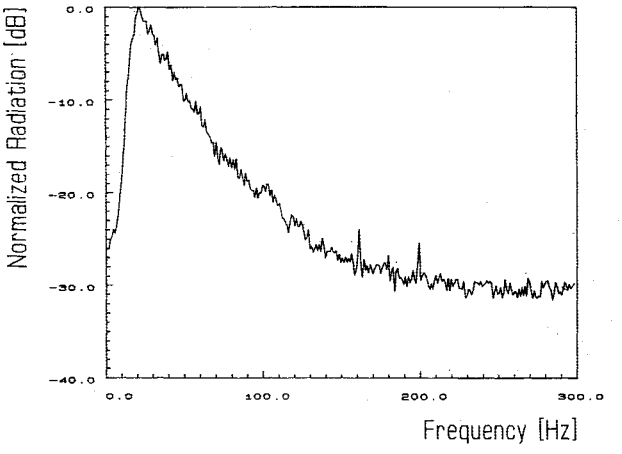

Fig. 6 Autospectrum of measured radiation (short duct).

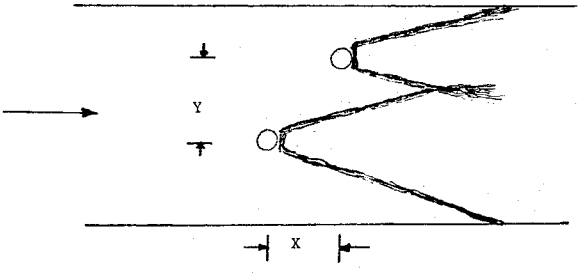

Fig. 7 Two flameholder combustor geometry.

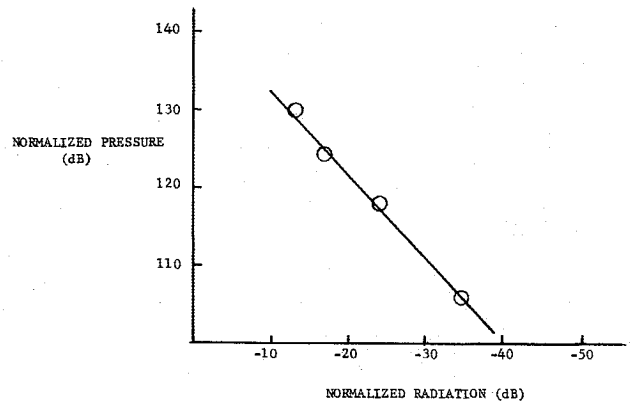

Fig. 8 Normalized radiation and corresponding normalized pressure levels for different flameholder displacements.

IV. Conclusion

A theoretical model capable of predicting the sound generated by confined flames has been developed and verified by comparison with experimental data. The relationship between the frequency contents of the unsteady flame heat release and the generated pressure spectra has been shown to depend upon the natural frequencies of the duct enclosing the flame. Finally, it has been shown experimentally that for low-velocity situations the flowfield influences the sound field only indirectly through its influence upon the combustion process.

References

[1]Waugh, R. C. and Brown, R. S., "A Literature Survey of Combustion Instability," CPIA Publication 375, April 1983, pp. 1-13.

[2]Zinn, B. T., "Pulsating Combustion," *Mechanical Engineering*, Vol. 107, Aug. 1985, pp. 36-41.

[3]Kumar, R. N., "Further Experimental Results on the Structure and Acoustics of Turbulent Jet Flames," *Aeroacoustics: Jet Noise, Combustion and Core Engine Noise*, edited by I. R. Schwartz, *Progress in Astronautics and Aeronautics*, Vol. 43, AIAA, New York, 1976, pp. 483-507.

[4]Hurle, I. R., Price, R. B., Sugden, T. M., and Thomas, A., "Sound Emission from Open Turbulent Premixed Flames," *Proceedings of the Royal Society of London: Mathematical and Physical Sciences*, Vol. 303, No. 1475, March 1968, pp. 409-428.

[5]Strahle, W. C., "A More Modern Theory of Combustion Noise," *Recent Advances in the Aerospace Sciences*, Edited by C. Casci, Plenum Press, New York, NY, 1985, pp. 103-114.

[6]Strahle, W. C., "On Combustion Generated Noise," *Journal of Fluid Mechanics*, Vol. 49, Pt. 2, Sept. 1971, pp. 399-414.

[7]Shivashankara, B. N., Strahle, W. C., and Handley, J. C., "Evaluation of Combustion Noise Scaling Laws by an Optical Technique," *AIAA Journal*, Vol. 13, May 1975, pp. 623-627.

[8]Barrere, M. and Williams, F. A., "Comparison of Combustion Instabilities Found in Various Types of Combustion Chambers," 12th Symposium (International) on Combustion, The Combustion Institute, Pittsburgh, PA, 1969, pp. 169-181.

[9]Poinsot, T., Hosseini, K., Le Chatlier, C., Candel, S. H., and Esposito, E., "An Experimental Analysis of Noise Sources in a Dump Combustor," *Dynamics of Reactive Systems Part I: Flames and Configurations,* Edited by J. R. Bowen, J. C. Leyer, and R. I. Soloukhin, Vol. 105, *Progress in Astronautics and Aeronautics,* AIAA, New York, NY, 1986, pp. 333-345.

[10]Hegde, U. G., Reuter, D., Zinn, B. T. and Daniel, B. R., "Fluid Mechanically Coupled Combustion Instabilities in Ramjet Combustors," AIAA Paper 87-0216, Jan. 1987.

[11]Goldstein, M. E., *Aeroacoustics*, McGraw-Hill, New York, NY, 1976. pp. 34-37.

[12]Morse, P. M. and Ingard, K. U., *Theoretical Acoustics*, McGraw-Hill, New York, NY, 1968, pp. 467-474.

[13]Hedge, U. G. and Strahle, W. C., "Sound Generation by Turbulence in Simulated Rocket Motor Cavities,"*AIAA Journal*, Vol. 23, Jan. 1985, pp. 71-76.

[14]Mehta, G. K., Ramachandra, M. K., and Strahle, W. C., "Correlation between Light Emission, Acoustic Emission, and Ion Density in Premixed Turbulent Flames," Eighteenth Symposium (International) on Combustion, The Combustion Institute, Pittsburgh, PA, 1980, pp. 1051-1059.

[15]Pierce, A. D., *Acoustics*, McGraw-Hill, New York, NY, 1981, pp. 532-534.